

Crystallization kinetics of polyethylene/paraffin oil blend sheets formed by thermally induced phase separation with different molecular weights of polyethylene

Junzhao Chen · Xiaobin Wang · Weijin Liu

Received: 16 March 2014 / Accepted: 10 July 2014 / Published online: 24 August 2014
© Akadémiai Kiadó, Budapest, Hungary 2014

Abstract Polyethylene/paraffin oil blend sheets with different molecular weights of polyethylene were prepared by thermally induced phase separation. Isothermal and non-isothermal crystallization behaviors of blend sheets were investigated by differential scanning calorimetry (DSC). Isothermal DSC curves were analyzed by Avrami equation, whereas non-isothermal DSC curves were analyzed by Jeziorny method and Mo method. Effective activation energy (ΔE) of isothermal and non-isothermal crystallization was calculated by Friedman method. Under isothermal condition, value of n in Avrami equation hovered at 2.1, and $\lg Z$ increased with the decrease of crystallization temperature. $\lg Z$ and ΔE of blend sheets with a larger molecular weight of polyethylene was smaller than that of blend sheets with smaller molecular weight. Under non-isothermal condition, value of n obtained by Jeziorny method hovered at 2.4, close to n of isothermal condition. $\lg Z_c$ increased with the increase of cooling rate and decrease of molecular weight of polyethylene. ΔE of different blend sheets were close to each other. Crystal structures of blend sheets formed under non-isothermal condition were analyzed by X-ray diffraction (XRD) analysis. XRD analysis showed that molecular weight of polyethylene and cooling rate had slight influence on

crystal structure and crystallinity of polyethylene/paraffin oil blend sheet.

Keywords Crystallization kinetics · Polyethylene · Paraffin oil

Introduction

Thermally induced phase separation (TIPS) is a widely used process for making polymeric microporous membranes as lithium-ion battery separators [1, 2]. In the process of TIPS, polyolefin resin is heated and melted with a low molecular weight substance, then the melt is extruded into a sheet while cooled down to be solidified. After the sheet is oriented biaxially, low molecular weight substance in the sheet is extracted with a volatile solvent to acquire micron-sized pores. The performance of the membrane obtained by TIPS will vary distinctly, with the solidification of polymer and the morphology formed during phase separation between polymer and the low molecular weight substance [3]. There are two kinds of phase separation in the process of TIPS, liquid–liquid phase separation [4–6] and solid–liquid phase separation [7–9], depending on the composition and the interaction between polymer and the low molecular weight substance. No matter which phase separation takes place, solidification of polymer caused by crystallization always occurs and has a significant effect on mechanical properties of the membrane.

Polyethylene (PE), as a material of most commercial lithium-ion battery separators [5, 10–13], provides a good mechanical property, chemical stability, thermal stability, and thermal shutdown capability. When polyethylene mixes with the solvent during the TIPS process, the solvent will influence the crystallinity and crystal structure of

J. Chen (✉) · W. Liu (✉)
School of Materials Science and Engineering, South China
University of Technology, Guangzhou 510640, China
e-mail: chenjunzhao@gmail.com

W. Liu
e-mail: pswjliu@scut.edu.cn

X. Wang
Foshan Jinhui Hi-tech Optoelectronic Material Co.Ltd,
Foshan 528000, China

polyethylene, so that it influences the properties of polyethylene membrane. Thus, it is important to understand the crystallization kinetics of polyethylene with the solvent. In general, crystallization kinetics of polymer is studied under isothermal and non-isothermal conditions. The Avrami equation [14] works well in describing isothermal crystallization behavior, especially at a low relative crystallinity. As to non-isothermal crystallization kinetics, Jeziorny [15], Ozawa [16], and Mo [17–19] propounded corresponding theory, respectively. Zhang et al. [20], investigated non-isothermal melt crystallization kinetics for ethylene-arylic acid copolymer in diluents by Jeziorny method, Ozawa method, and Mo method. Wang et al. [21], analyzed non-isothermal crystallization kinetics of high density polyethylene/titanium dioxide composites using Jeziorny and Mo methods.

In this paper, isothermal and non-isothermal crystallization kinetics of polyethylene/paraffin oil blend sheets with different weight-average molecular weights of polyethylene were analyzed. Firstly, exothermic curves of different polyethylene/paraffin oil blend sheets were obtained by differential scanning calorimeter (DSC). Based on exothermic curves, Avrami equation was used to analyze isothermal crystallization, while Jeziorny method and Mo method were used to analyze non-isothermal crystallization. Then, effective activation energy of polyethylene/paraffin oil blend sheet was calculated by Friedman method [22, 23]. At last, X-ray diffraction analysis was used to investigate the crystal structure and crystallinity of polyethylene/paraffin oil blend sheets.

Experimental

Materials

Polyethylene of different weight-average molecular weights (3×10^5 , 5×10^5 , and 1×10^6 , whose densities are 0.950, 0.941, and 0.952 g cm^{-3} , respectively) were purchased from Sinopec Maoming Company (China). Paraffin oil (boiling point above $271 \text{ }^\circ\text{C}$, density between 0.845 and 0.890 g mL^{-1}) was purchased from Tianjin Kaiwei and Yongli United Chemical Company (China).

Preparation of polyethylene/paraffin oil blend sheets

Polyethylene/paraffin oil blend sheets with 30 % mass of polyethylene were prepared by an extruder (TES-35B, Nanjin Ruiya Polymer Processing Equipment Limited) with melting temperature around $200 \text{ }^\circ\text{C}$ and screw rotation speed at 200 rpm. All sheets were quenched to $20 \text{ }^\circ\text{C}$ to be solidified.

Differential scanning calorimetry (DSC) measurement

Differential scanning calorimeter (DSCAQ20, TA Instruments) was adopted to analyze melting behaviors, non-isothermal and isothermal crystallization kinetics of polyethylene/paraffin oil blend sheets. Crystallinity of blend sheet (X_{DSC}) was calculated by Eq. 1:

$$X_{\text{DSC}} = \frac{\Delta H}{\phi \Delta H_f^*} \times 100 \%, \quad (1)$$

where ΔH is the enthalpy of the crystallization or melting process, ΔH_f^* is the enthalpy of polyethylene with a crystallinity of 100 %, whose value is 277.1 J g^{-1} in the literature [24], and ϕ is the mass fraction of polyethylene in the blend sheet.

Melting behaviors

Three kinds of neat polyethylene and polyethylene/paraffin oil blend sheets were sealed in aluminum pans, respectively. All the samples were heated from room temperature to $160 \text{ }^\circ\text{C}$ at a controlled rate of $10 \text{ }^\circ\text{C min}^{-1}$. DSC curves which include the information about melting behaviors were obtained.

Isothermal crystallization

Each polyethylene/paraffin oil blend sheet was sealed in an aluminum pan. According to literatures [21, 25], samples were heated from room temperature to $160 \text{ }^\circ\text{C}$ at a controlled rate of $100 \text{ }^\circ\text{C min}^{-1}$ and kept at $160 \text{ }^\circ\text{C}$ for 5 min to erase the prehistory, and then quenched to predetermined temperature at $100 \text{ }^\circ\text{C min}^{-1}$. Each sample was kept at corresponding temperature until the DSC curve, as a function of time, was obtained.

Non-isothermal crystallization

Each polyethylene/paraffin oil blend sheet was sealed in an aluminum pan, heated from room temperature to $160 \text{ }^\circ\text{C}$ at a controlled rate of $100 \text{ }^\circ\text{C min}^{-1}$ and kept at $160 \text{ }^\circ\text{C}$ for 5 min, and then cooled to room temperature at a controlled rate of 1, 3, 5, and $10 \text{ }^\circ\text{C min}^{-1}$, respectively. DSC curves, as function of time and temperature, were obtained.

X-ray diffraction (XRD) analysis

Polyethylene/paraffin oil blend sheets with different molecular weights of polyethylene were heated to $160 \text{ }^\circ\text{C}$ at a controlled rate of $100 \text{ }^\circ\text{C min}^{-1}$, kept at $160 \text{ }^\circ\text{C}$ for 5 min, and then cooled to room temperature at a controlled rate of 1 and $10 \text{ }^\circ\text{C min}^{-1}$, respectively, at last flattened and trimmed

Table 1 Melting parameters derived from DSC curves for neat polyethylene and blend sheets

Molecular weight	Samples	$T_m^{on}/^{\circ}C$	$T_m^p/^{\circ}C$	$T_m^e/^{\circ}C$	Crystallinity/ %
3×10^5	Neat polyethylene	125.4	132.4	136.5	49.5
	Blend sheet	115.0	123.1	127.0	60.3
5×10^5	Neat polyethylene	132.6	140.7	145.9	56.2
	Blend sheet	115.7	124.9	128.6	67.3
1×10^6	Neat polyethylene	133.1	141.2	146.0	53.9
	Blend sheet	115.5	123.6	127.5	60.3

into circular samples with a diameter of 10 mm. Crystal structures of samples were analyzed by X-ray diffractometer (D/max-III A, Rigaku Industrial Corporation) using nickel-filtered Cu K α source. The scanning range was from 0 $^{\circ}$ to 60 $^{\circ}$ with a scanning velocity of 8 $^{\circ}$ min $^{-1}$ at a voltage of 40 kV and a filament current of 30 mA.

Results and discussion

Melting behaviors

Melting behaviors of polyethylene/paraffin oil blend sheets were investigated, melting point (T_m^p), onset melting temperature (T_m^{on}), and end melting temperature (T_m^e) are listed in Table 1. T_m^p , T_m^{on} , and T_m^e of polyethylene/paraffin oil blend sheet are lower than corresponding neat polyethylene, because existence of paraffin oil leads to loose crystal structure with less heat-resisting ability. As shown in Table 1, melting point of neat polyethylene increases with the increase of molecular weight, but that of blend sheet changes very little. This can be ascribed to the similar crystal structure formed in different kinds of blend sheets owning almost the same heat-resisting ability. On the other hand, crystallinity of blend sheet is larger than corresponding neat polyethylene, which can be attributed to the fact that molecular chains of paraffin oil act as heterogeneous nucleating agents which induce nucleation of polyethylene and increase the crystallinity of polyethylene in blend sheet.

Isothermal crystallization

DSC curves of isothermal crystallization of polyethylene/paraffin oil blend sheets with different molecular weights of polyethylene are illustrated in Fig. 1. As shown in Fig. 1, while crystallization temperature (T_c) decreases, exothermic peak becomes narrow and the time to finish the crystallization becomes shorter. Moreover, polyethylene, with a larger molecular weight, needs more time to reach max crystallinity, due to the less free movement of polyethylene molecular chains.

The relative crystallinity (X_t) is defined as follows:

$$X_t = \frac{\int_{t_0}^t (dH_c/dt)dt}{\int_{t_0}^{t_{\infty}} (dH_c/dt)dt}, \quad (2)$$

where the t_0 and t_{∞} are the parameters of time when crystallization begins and ends, dH_c is the change of enthalpy during an infinitesimal time range dt around time t . According to the definition of X_t , value of X_t can be calculated by integrating DSC curve which is a function of time. Curves of isothermal relative crystallinity varying with time are shown in Fig. 2. It is clear that crystallization time when relative crystallinity reaches 100 % becomes longer as T_c increasing, and variation of crystallization time caused by increase of T_c becomes larger while molecular weight of polyethylene increasing. Besides, all the scatter plots in Fig. 3 are S-curve which indicates that crystallization rates at the beginning and end of crystallization are slower than the other period. Generally, at the beginning of crystallization, nucleation of crystalline slows down crystallization rate. And at the end of crystallization, impingement of adjacent crystalline restricts growth of spherulites.

Avrami equation

Avrami equation shown as follows is widely used to analyze isothermal crystallization of polymer [14].

$$X_t = 1 - \exp(-Zt^n) \quad (3)$$

$$\lg[-\ln(1 - X_t)] = n \lg t + \lg Z. \quad (4)$$

Z is the composite constant of crystallization rate of which the value is related to the nucleation rate and growth rate of crystal, n is the Avrami exponent whose value depends on the way how nucleus forms and how crystal grows. By transforming the horizontal axis from t to $\lg t$ and the vertical axis from X_t to $\lg[-\ln(1 - X_t)]$, Fig. 2 changed into Fig. 3. In Fig. 3, data distribution of each scatter plot is near linear. In particular, two stages of relative crystallinity observed in the other research [26] do not appear in this paper, which may be caused by relative simple crystallization structure. All scatter plots in Fig. 3 were linearly fitted (with iteration fitting, *Adjust* $r^2 > 0.99099$).

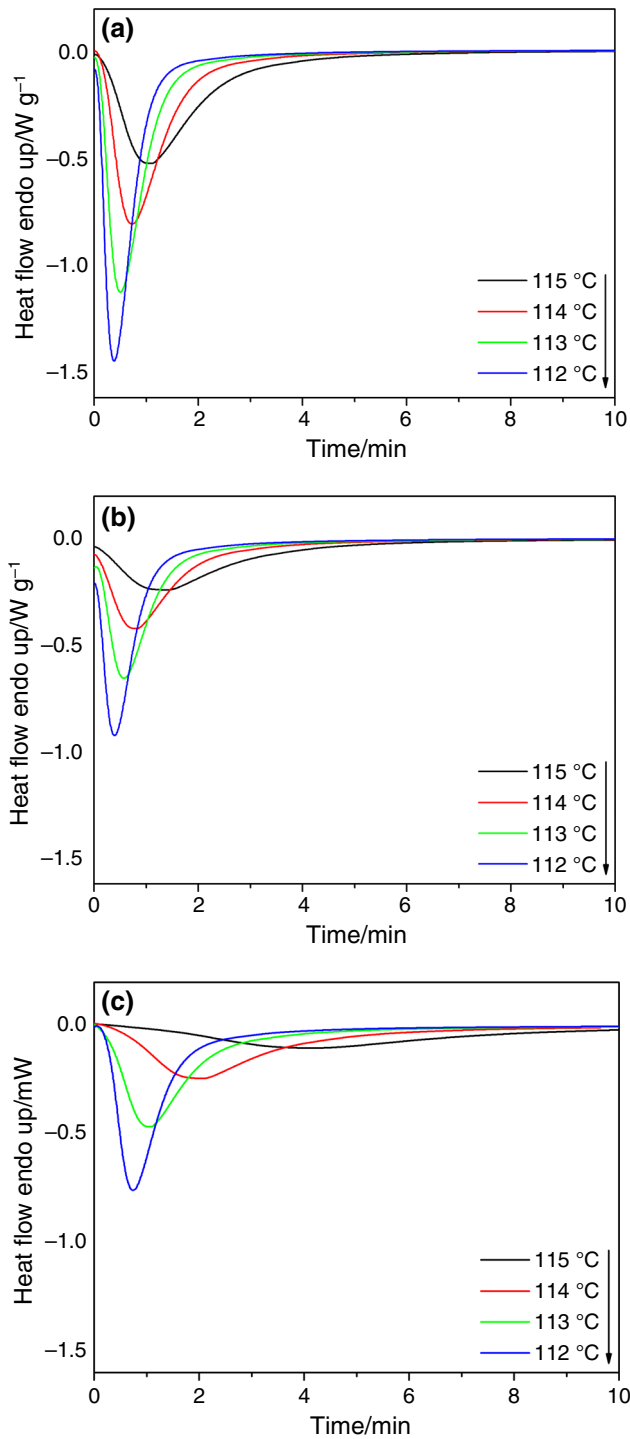


Fig. 1 Isothermal DSC curves of PE/paraffin oil blend sheets with different molecular weights of PE: **a** 3×10^5 ; **b** 5×10^5 ; **c** 1×10^6

Referring to Eq. 4, slope of each line is n and interception of each line is $\lg Z$. Values of n and $\lg Z$ are listed in Table 2. As seen in Table 2, most values of n are between 2 and 3. Theoretically, in heterogeneous nucleation, value of n equal to 2 indicates formation of two-dimensional crystal structure (lamellae) and equal to 3 indicates

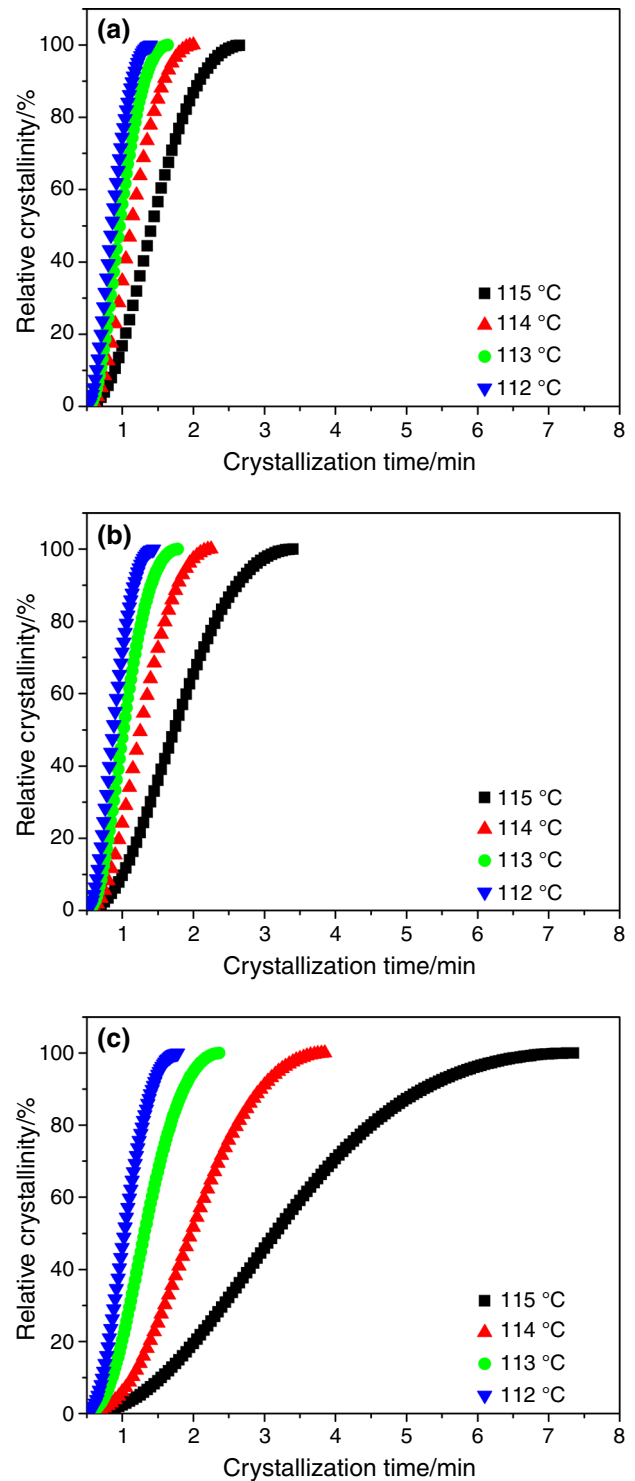


Fig. 2 Curves of isothermal relative crystallinity varying with crystallization time for PE/paraffin oil blend sheets with different molecular weights of PE: **a** 3×10^5 ; **b** 5×10^5 ; **c** 1×10^6

formation of three-dimensional crystal structure (spherulites). Non-integer value between 2 and 3 could be attributed to complicate the situation of nucleation and growth of crystal, that is, both lamellae and spherulites are formed

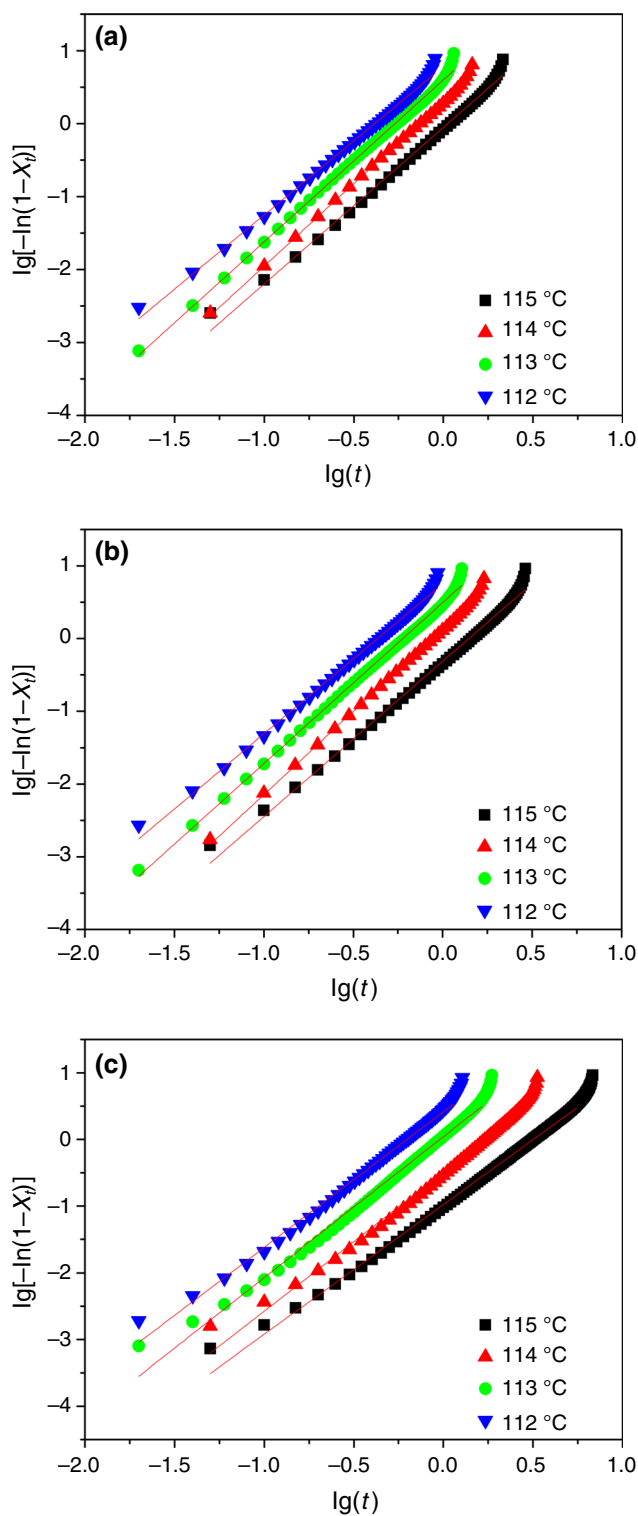


Fig. 3 Plots of $\lg[-\ln(1-X_t)]$ versus $\lg(t)$ for isothermal crystallization of PE/paraffin oil blend sheets with different molecular weights of PE: **a** 3×10^5 ; **b** 5×10^5 ; **c** 1×10^6

during the crystallization process. Furthermore, variation of n with increase of T_c is negligible, which demonstrates that temperature between 115 and 112 °C has slight

Table 2 Isothermal crystallization kinetics parameters derived from DSC curves by Avrami equation

Molecular weight	$T_c/^\circ\text{C}$	n	Z	$Adj.r^2$
3×10^5	115	2.15	0.890	0.99258
	114	2.26	2.043	0.99773
	113	2.22	3.990	0.99687
	112	2.03	6.060	0.99483
5×10^5	115	2.14	0.488	0.99258
	114	2.29	1.381	0.99773
	113	2.21	3.120	0.99687
	112	2.06	5.639	0.99483
1×10^6	115	1.95	0.106	0.99634
	114	2.09	0.324	0.99099
	113	2.11	1.102	0.99248
	112	2.04	2.611	0.99429

influence on crystallization structure of polyethylene in blend sheet. $\lg Z$ increases while crystallization temperature decreases, indicating that crystallization rate becomes faster at a lower temperature, which is reasonable for crystallization proceeding between melting point and temperature where maximum crystallization rate exists. Crystallization of polyethylene includes nucleation and crystal growth. Decrease of crystallization temperature contributes to nucleation but impedes crystal growth, which results in maximum crystallization rate whose crystallization temperature is T_{max} . While the crystallization temperature is between melting point and T_{max} (crystallization temperatures in this paper are within this range), crystallization rate depends mostly on nucleation. Decrease of crystallization temperature is conducive to nucleation and therefore facilitates increase of crystallization rate. On the other hand, $\lg Z$ decreases while molecular weight of polyethylene increases, because polyethylene of a larger molecular weight has longer molecular chains to move and fold when molecules move from diluent to crystal lattice.

Crystallization half-time ($t_{1/2}$) is defined as the time when relative crystallinity reaches 50%. Value of $t_{1/2}$ usually indicates how fast the crystal grows. The larger the value of $t_{1/2}$ is, the slower the crystal grows. Value of $t_{1/2}$ can be easily acquired by reading data of curves in Fig. 3 directly or by calculation using Eq. 5.

$$t_{1/2} = \left(\frac{\ln 2}{Z}\right)^{1/n} \tag{5}$$

Figure 4 shows how crystallization half-time of blend sheet varies with crystallization temperature. The higher the crystallization temperature is, the larger the value of crystallization half-time will be and the slower the crystal grows. The larger the molecular weight of polyethylene is, the larger the value of crystallization half-time will be and

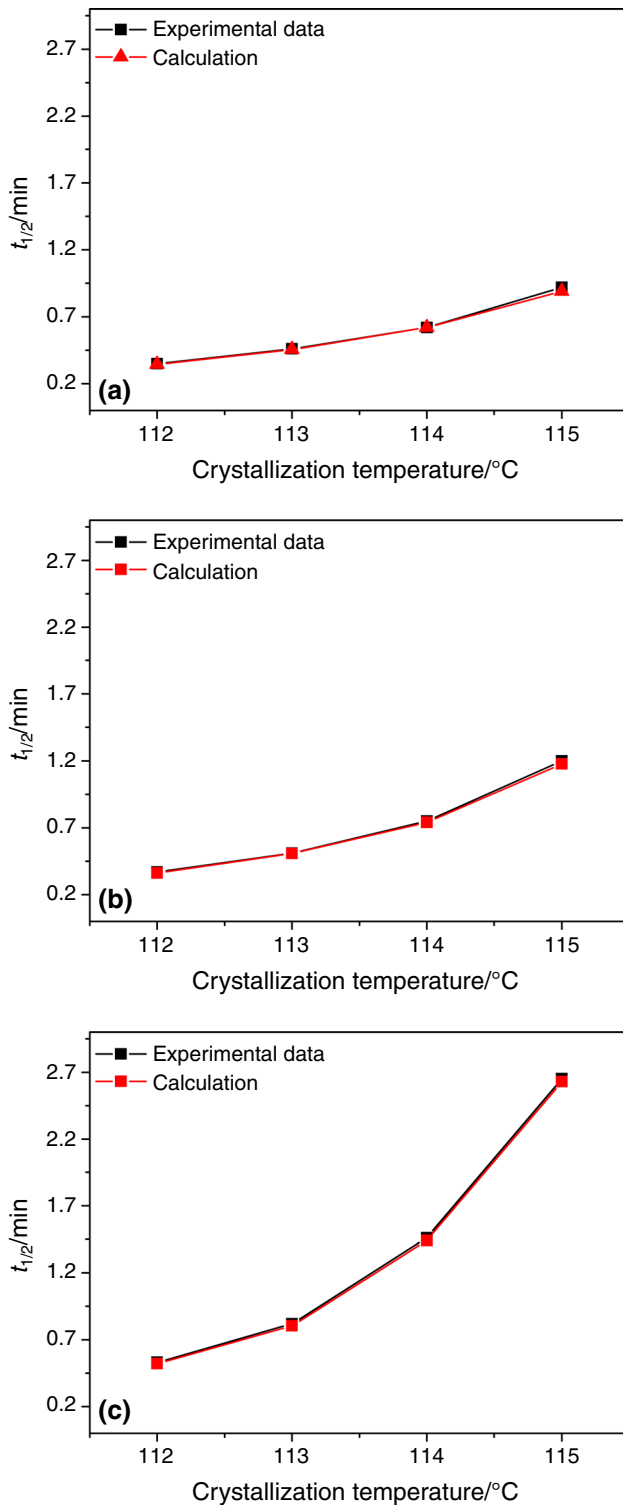


Fig. 4 Plots of isothermal crystallization half-time versus crystallization temperature for PE/paraffin oil blend sheets with different molecular weights of PE: **a** 3×10^5 ; **b** 5×10^5 ; **c** 1×10^6

the slower the crystallization rate is. Moreover, the crystallization half-time by calculation is so close to the crystallization half-time derived from experiment data, which

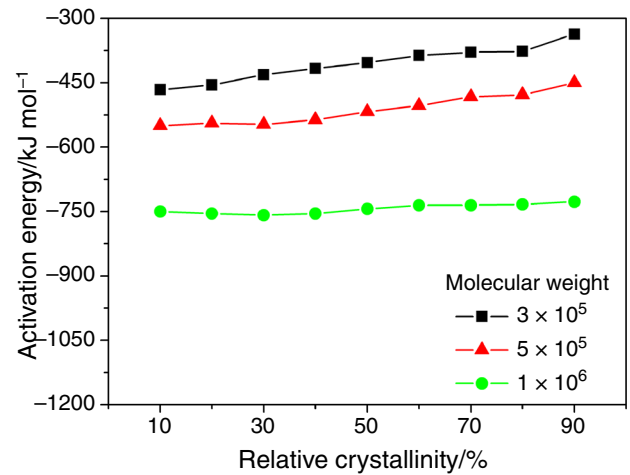


Fig. 5 Activation energy of isothermal crystallization for PE/paraffin oil blend sheets with different molecular weights of PE

shows that Avrami equation does well in analyzing isothermal crystallization.

Crystallization activation energy

Crystallization activation energy (ΔE) is usually regarded as an experimentally determined parameter that indicates the sensitivity of the crystallization rate to temperature, the larger the absolute value of ΔE is, the more sensitive to temperature crystallization rate would be. In this paper, the effective activation energy was calculated by Friedman method given as follows [22, 23].

$$\ln\left(\frac{dX_t}{dt}\right)_{X_t} = A - \frac{\Delta E}{RT} \quad (6)$$

A is pre-exponential constant, R is the universal gas constant ($8.314 \text{ J mol}^{-1} \text{ K}^{-1}$), and dX_t is the change of X_t during an infinitesimal time range dt around time t when relative crystallinity is X_t . According to Eq. 6, ΔE of a given X_t is just the slope of the line acquired by plotting $\ln(dX_t/dt)$ against $1/T$. Different dependences of ΔE on X_t of polyethylene/paraffin oil blend sheets with different molecular weights of polyethylene in isothermal process are shown in Fig. 5. Values of all crystallization activation energy are negative, which indicate that crystallization rate decreases with increasing temperature. With molecular weight of polyethylene increasing, the effective activation energy decreases, indicating that the crystallization rate of blend sheet with a larger molecular weight of polyethylene is more susceptible to temperature (variation of crystallization rate with increase of temperature is larger). On the other hand, the effective activation energy increases gradually while X_t increases from 10 to 90 %, which demonstrates that crystallization rate at the beginning of

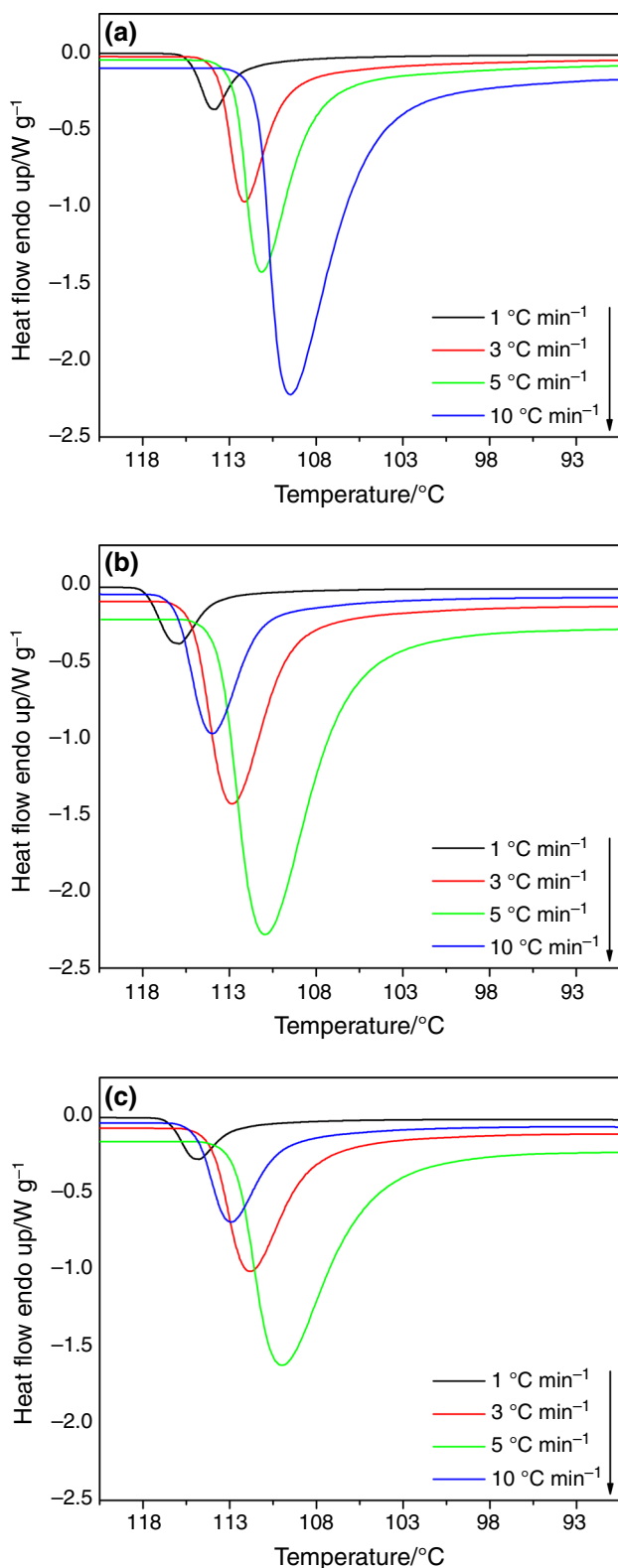


Fig. 6 Non-isothermal DSC curves of PE/paraffin oil blend sheets with different molecular weights of PE: **a** 3×10^5 ; **b** 5×10^5 ; **c** 1×10^6

Table 3 Parameters of non-isothermal DSC curves of PE/paraffin oil blend sheets

Molecular weight	$\Phi/^\circ\text{C min}^{-1}$	$T_c^{\text{on}}/^\circ\text{C}$	$T_c^{\text{p}}/^\circ\text{C}$	$T_c^{\text{e}}/^\circ\text{C}$	$\Delta T_c/^\circ\text{C}$	$\Delta H/\text{J g}^{-1}$
3×10^5	1	114.8	113.3	111.7	3.2	61.66
	3	113.4	111.6	109.3	4.0	65.40
	5	112.3	110.6	107.6	4.6	65.44
	10	111.0	109.0	104.5	6.5	64.13
5×10^5	1	117.3	115.4	113.4	3.9	66.07
	3	115.6	113.5	110.8	4.8	67.84
	5	114.7	112.3	109.0	5.6	68.19
	10	113.2	110.4	105.7	7.5	67.16
1×10^6	1	116.0	114.3	112.2	3.8	49.34
	3	114.5	112.4	109.6	4.9	49.55
	5	113.6	111.3	107.8	5.8	49.19
	10	112.7	109.4	104.6	8.1	50.11

crystallization is more easily influenced by temperature than that at the end of crystallization.

Non-isothermal crystallization

DSC curves of non-isothermal crystallization of polyethylene/paraffin oil blend sheets with different molecular weights of polyethylene are illustrated in Fig. 6. Onset crystallization temperature (T_c^{on}), peak temperature of crystallization (T_c^{p}), and end crystallization temperature (T_c^{e}) of each curve are listed in Table 3. While cooling rate increases, positions of all exothermic peak shift to lower temperature (values of T_c^{on} , T_c^{p} , and T_c^{e} decrease), all exothermic peaks become wider (value of ΔT_c increases, where $\Delta T_c = T_c^{\text{on}} - T_c^{\text{e}}$), but ΔH of blend sheet changes very little. Furthermore, ΔH of blend sheet with polyethylene of a molecular weight of 1×10^6 is smaller than that of other blend sheets, meaning that polyethylene of a molecular weight of 1×10^6 has a much lower crystallinity under the same non-isothermal condition.

Curves of non-isothermal relative crystallinity varying with time are shown in Fig. 7. All scatter plots in Fig. 7 are distributed in S-shape, same as isothermal condition. With increase of cooling rate, crystallization time to reach maximum relative crystallinity becomes shorter. Under non-isothermal condition, crystallization time to reach maximum relative crystallinity does not change too much with increase of molecular weight of polyethylene, compared with isothermal condition.

Jeziorny method

In order to analyze non-isothermal crystallization kinetics, Jeziorny modified Avrami equation to take the cooling rate

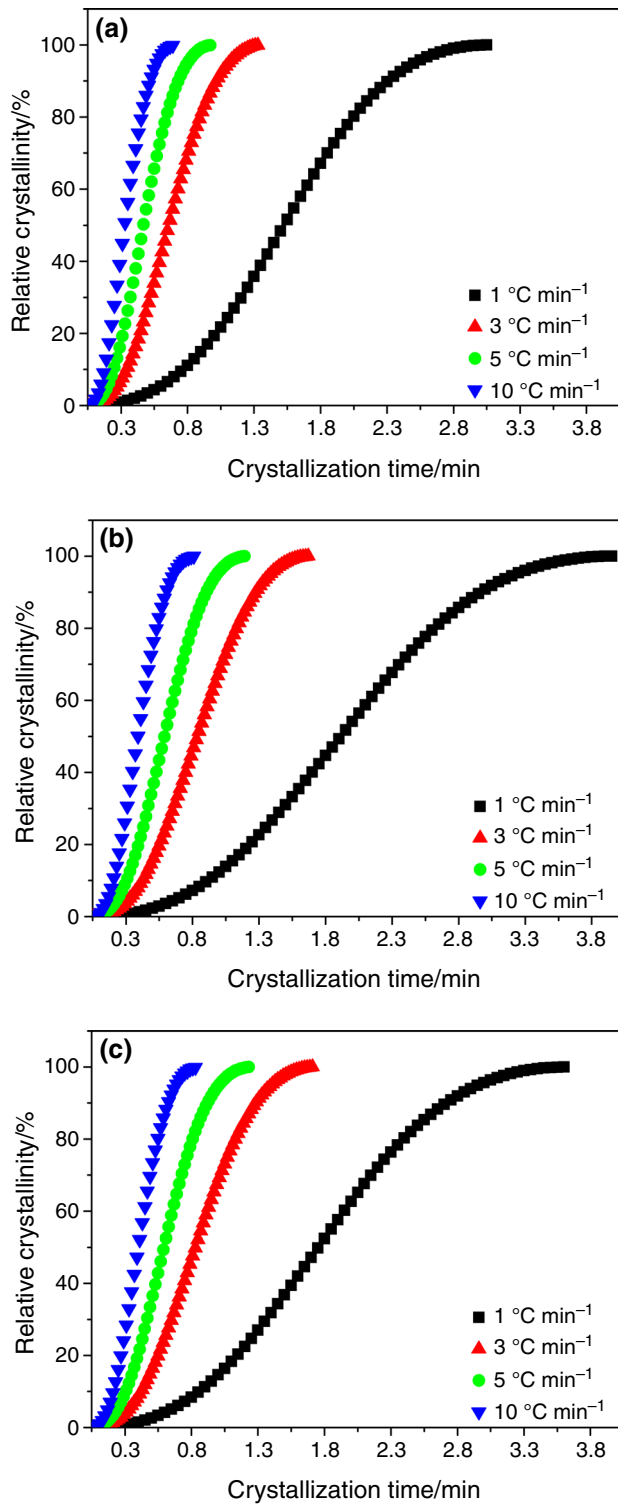


Fig. 7 Curves of non-isothermal relative crystallinity varying with crystallization time for PE/paraffin oil blend sheets with different molecular weights of PE: **a** 3×10^5 ; **b** 5×10^5 ; **c** 1×10^6

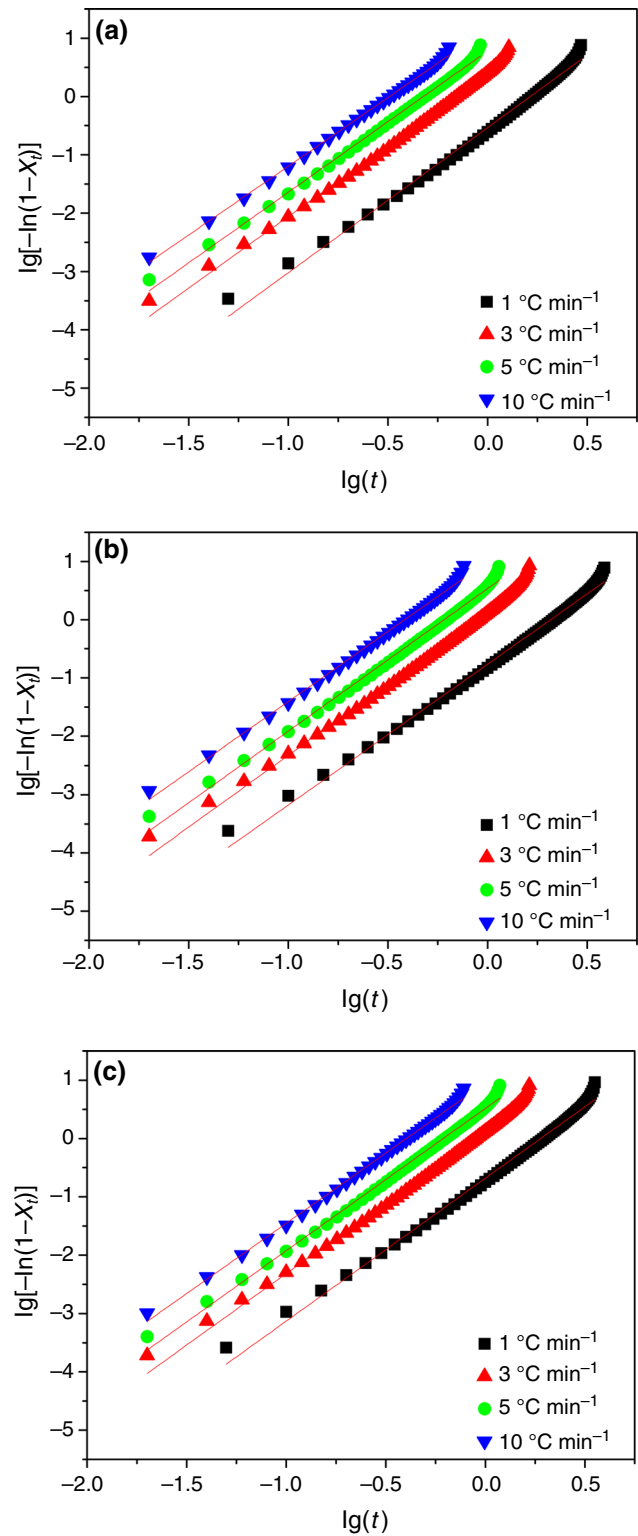


Fig. 8 Plots of $\lg[-\ln(1-X_t)]$ versus $\lg(t)$ for non-isothermal crystallization of PE/paraffin oil blend sheets with different molecular weights of PE: **a** 3×10^5 ; **b** 5×10^5 ; **c** 1×10^6

Table 4 Non-isothermal crystallization kinetics parameters derived from DSC curves by Jeziorny method

Molecular weight	$\Phi/^\circ\text{C min}^{-1}$	n	Z_t	Z_c	$Adj.r^2$
3×10^5	1	2.43	0.280	0.280	0.99186
	3	2.43	2.610	1.377	0.99346
	5	2.39	5.830	1.423	0.99504
	10	2.32	13.747	1.300	0.99703
5×10^5	1	2.41	0.172	0.172	0.99376
	3	2.46	1.382	1.114	0.99326
	5	2.45	3.420	1.279	0.99470
	10	2.40	9.961	1.258	0.99589
1×10^6	1	2.45	0.209	0.209	0.99299
	3	2.45	1.371	1.111	0.99484
	5	2.44	3.285	1.269	0.99567
	10	2.41	9.007	1.246	0.99723

of non-isothermal condition into account. Avrami equation was modified as follows [15]:

$$\lg[-\ln(1 - X_t)] = n \lg t + \lg Z_t \tag{7}$$

$$\lg Z_c = \frac{\lg Z_t}{\Phi}, \tag{8}$$

where Z_c , same as Z in Avrami equation, is the composite constant of crystallization rate and Φ is the cooling rate.

After transforming the horizontal axis from t to $\lg t$ and the vertical axis from X_t to $\lg[-\ln(1-X_t)]$, Fig. 7 was converted to Fig. 8. Data scattered in Fig. 8 were linearly fitted (with iteration fitting, $Adjust\ r^2 > 0.99186$). Slope of each line is n and interception of each line is $\lg Z_t$. Values of n , $\lg Z_t$, and $\lg Z_c$ are listed in Table 4. Value of n hovers at 2.4 and change little with the increase of cooling rate and molecular weight of polyethylene, indicating that different blend sheets share almost the same crystallization structure (a combination of two-dimensional structure and three-dimensional structure). Value of $\lg Z_c$ increases the with increase of cooling rate, which demonstrates that crystallization rate becomes faster at a larger cooling rate. Besides, value of $\lg Z_c$ decreases with the increase of molecular weight of polyethylene, which can be attributed to the decline of ability to move and shift molecular chains.

Values of $t_{1/2}$ acquired by calculation and reading data of curves in Fig. 7 directly are shown in Fig. 9. Value of $t_{1/2}$ by calculation is almost equal to that obtained from experiment data, that is, Jeziorny method is capable of analyzing crystallization under non-isothermal condition. Moreover, while cooling rate increases, $t_{1/2}$ decreases, in other words, crystallization rate increases. On the other hand, $t_{1/2}$ of blend sheet with polyethylene of a molecular weight of 3×10^5 is smaller compared with other two

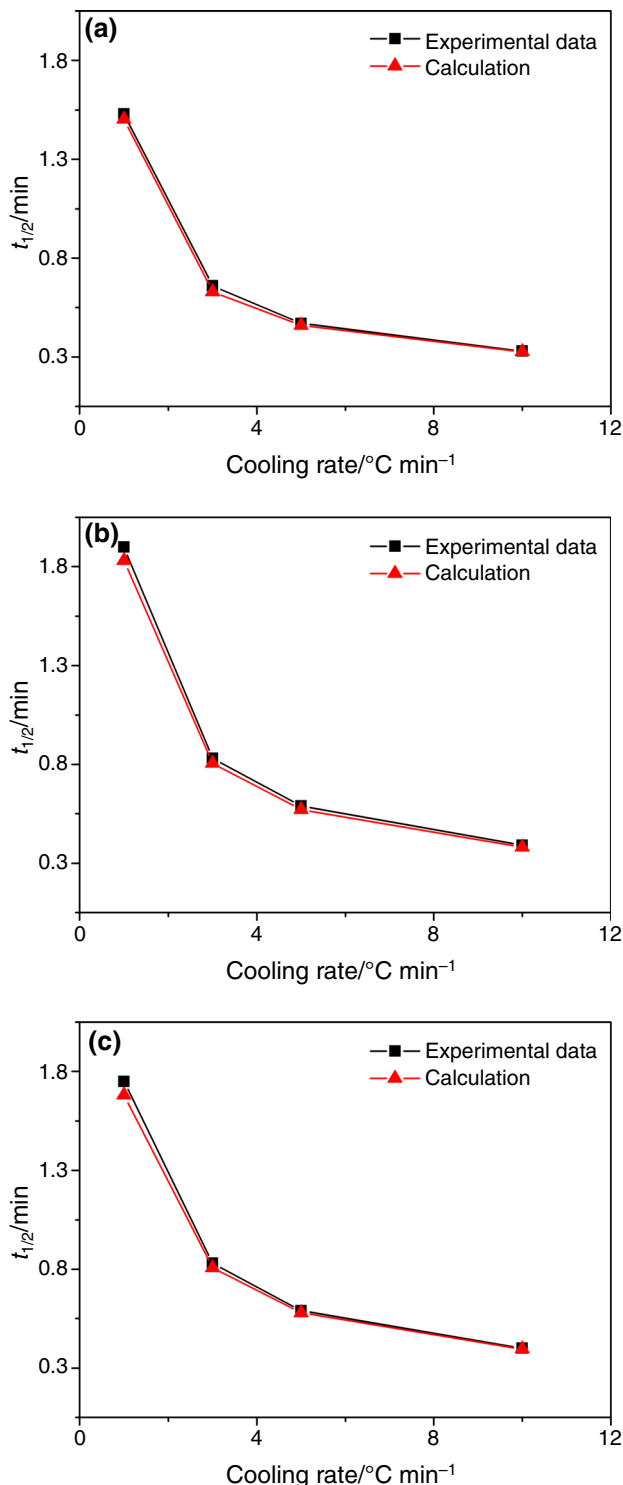


Fig. 9 Plots of non-isothermal crystallization half-time versus cooling rate for PE/paraffin oil blend sheets with different molecular weights of PE: **a** 3×10^5 ; **b** 5×10^5 ; **c** 1×10^6

blend sheets, indicating that crystallization of it proceeds at a faster speed, which is consistent with the result coming from analysis of $\lg Z_c$.

Mo method

Based on the theory of Evens and Avrami equation, Ozawa proposed a new equation to analyze non-isothermal crystallization kinetics of polymer [16].

$$1 - X(T) = \exp[-K(T)/\Phi^m] \quad (9)$$

$$\lg[-\ln(1 - X(T))] = \lg K(T) - m \lg \Phi. \quad (10)$$

$X(T)$ is the relative crystallinity at the temperature T , m is the Ozawa index whose value depends on the structure of crystalline, and $\lg K(T)$, as a function of temperature, varies with the way how nucleus forms, how nucleus grows and how fast growth rate is.

Mo method [17–19] combined Jeziorny method and Ozawa method, and made some mathematical transformations as follows: at a given time (t) (corresponding temperature of it is T), the equation below holds.

$$X_t = X(T) \quad (11)$$

$$\lg[-\ln(1 - X_t)] = \lg[-\ln(1 - X(T))]. \quad (12)$$

According to Ozawa method and Jeziorny method, Eq. 13 can be deduced from Eq. 12.

$$n \lg t + \lg Z_t = \lg K(T) - m \lg \Phi \quad (13)$$

$$\lg \Phi = \lg[K(T)/Z_t]^{1/m} - (n/m) \lg t \quad (14)$$

$$\lg \Phi = \lg F(T) - a \lg t. \quad (15)$$

$F(T) = [K(T)/Z_t]^{1/m}$, $a = n/m$. $F(T)$, as a function of temperature, depends on the rate of crystallization. The higher the value of $F(T)$ is, the slower the crystal grows. Analysis of non-isothermal crystallization by Mo method was carried out at four given relative crystallinity (20, 40, 60, and 80 %). Scatter plots in Fig. 10 were obtained by plot $\lg \Phi$ against $\lg t$. Data scattered in Fig. 10 were linearly fitting (with iteration fitting, $Adjusted\ r^2 > 0.99120$). According to Eq. 15, slope of the fitting line is a and interception of the fitting line is $\lg F(T)$. Values of a and $\lg F(T)$ are listed in Table 5. $\lg F(T)$ increases with the increase of relative crystallinity, meaning that it gets harder for crystallization at a larger relative crystallinity. Values of a do not change very much along with increase of relative crystallinity, indicating that crystallization structure formed at different relative crystallinity seems to be similar. Blend sheet with polyethylene of a molecular weight of 3×10^5 has the smallest $\lg F(T)$, which could be contributed to freer movement of molecular chains. $\lg F(T)$ of blend sheet with polyethylene of a molecular weight of 1×10^6 is even smaller than that of blend sheet with polyethylene of a molecular weight of 5×10^5 , which can be ascribed to the crystallinity of polyethylene. Crystallinity of polyethylene could be inferred from value of ΔH . ΔH of polyethylene with molecular weight of 5×10^5 is around 67 J g^{-1} , in

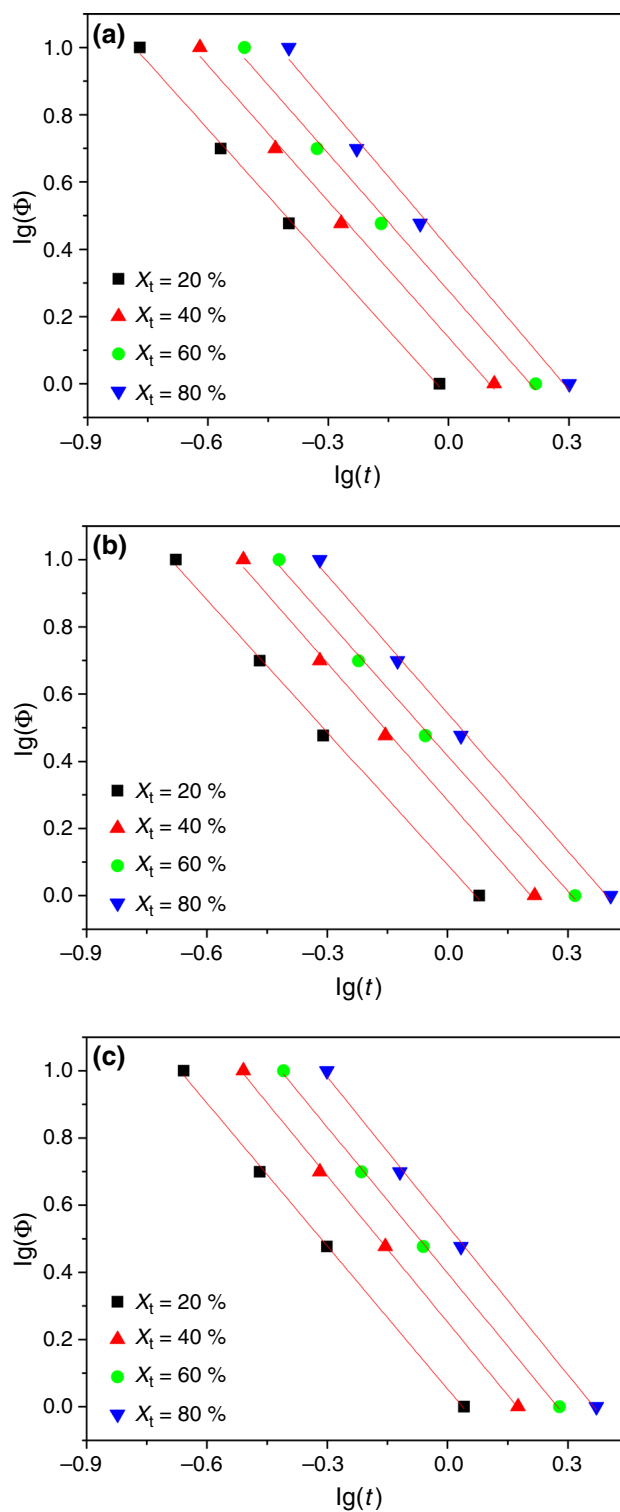
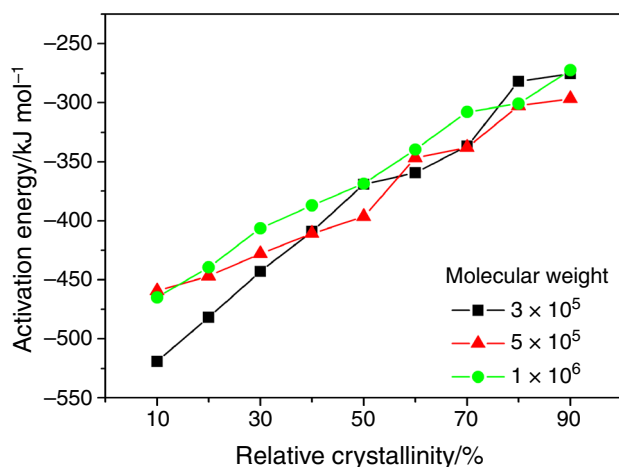


Fig. 10 Plots of $\lg(\Phi)$ versus $\lg(t)$ for PE/paraffin oil blend sheets with different molecular weights of PE: **a** 3×10^5 ; **b** 5×10^5 ; **c** 1×10^6

the meantime, ΔH of polyethylene with molecular weight of 1×10^6 is around 50 J g^{-1} . Thus, crystallinity of two kinds of polyethylene differ widely, which makes $\lg F(T)$ of each blend sheet incomparable.

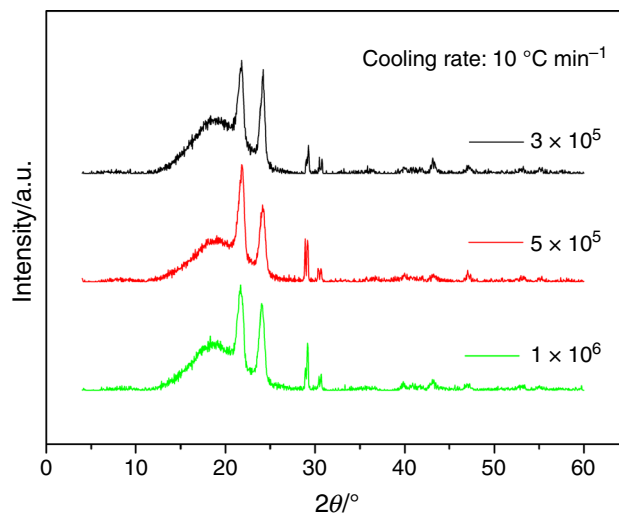
Table 5 Non-isothermal crystallization kinetics parameters derived from DSC curves by Mo method

Molecular weight	$X_t/\%$	a	$F(T)$	$Adj.r^2$
3×10^5	20	1.33	0.913	0.99768
	40	1.35	1.374	0.99476
	60	1.36	1.892	0.99248
	80	1.41	2.538	0.99120
5×10^5	20	1.32	1.234	0.99717
	40	1.36	1.920	0.99613
	60	1.34	2.609	0.99743
	80	1.37	3.489	0.99650
1×10^6	20	1.42	1.129	0.99834
	40	1.45	1.785	0.99901
	60	1.45	2.496	0.99917
	80	1.48	3.453	0.99785

**Fig. 11** Activation energy of non-isothermal crystallization for PE/paraffin oil blend sheets with different molecular weights of PE

Crystallization activation energy

Different dependences of ΔE on X_t of polyethylene/paraffin oil blend sheets with different molecular weights of polyethylene in non-isothermal process are shown in Fig. 11. Same as isothermal condition, ΔE increases gradually when X_t grows from 10 to 90 %, which indicates that crystallization rate at lower relative crystallinity is more sensitive to change of temperature than that at higher relative crystallinity. ΔE of different blend sheets are more or less the same. But ΔE of blend sheet with polyethylene of a molecular weight of 1×10^6 is larger than other two blend sheets in the whole range, which indicates that crystallization rate of polyethylene with a molecular weight of 1×10^6 is less susceptible to temperature. Polyethylene of a molecular weight of 1×10^6 has longest molecular chains and worse movement capacity, which causes a lack

**Fig. 12** XRD patterns for polyethylene/paraffin oil blend sheets formed under a cooling rate of $10 \text{ }^\circ\text{C min}^{-1}$

of time for crystallization of polyethylene at four given cooling rates. Thus, variation of the crystallization rate of polyethylene of molecular weight of 1×10^6 is smaller than other two blend sheets.

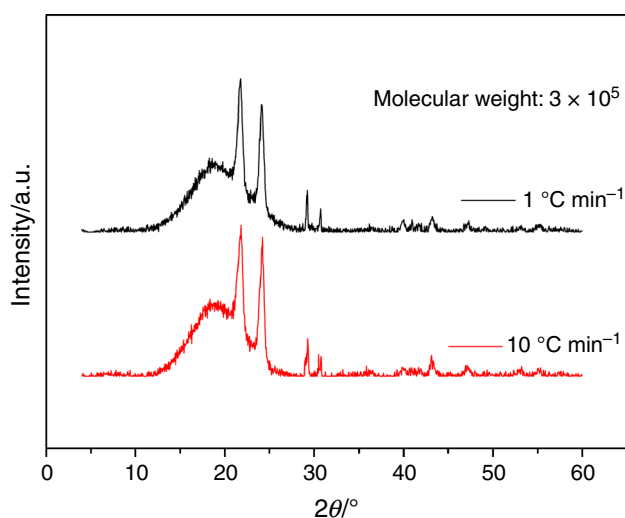
Activation energy of non-isothermal crystallization differs from that of isothermal crystallization in values and trends, because there is a tremendous difference in temperature condition of two processes. Isothermal crystallization proceeds at a constant temperature between 112 and 115 °C, but non-isothermal crystallization proceeds in a larger temperature range (between 105 and 117 °C). Thus at the same crystallinity, crystallization rate and crystallization temperature of isothermal crystallization differ from those of non-isothermal crystallization, which results in the difference of values and trends of activation energy for two processes (see Eq. 6). On the other hand, isothermal crystallization starts and finishes at a constant temperature, but non-isothermal crystallization proceeds under dynamic condition where larger degree of under cooling exists. While larger degree of under cooling exists, when crystallization temperature changes, variations of non-isothermal crystallization rate of different blend sheets are close to each other. That is, sensitivities of non-isothermal crystallization rate to temperature for different blend sheets are almost the same.

Crystal structure under non-isothermal condition

XRD patterns of polyethylene/paraffin oil blend sheets with different molecular weights of PE which were formed under a cooling rate of $10 \text{ }^\circ\text{C min}^{-1}$ are illustrated in Fig. 12. Two obvious diffractive peaks which appear around 21.7° and 24.1° correspond to typical crystal plane

Table 6 XRD parameters of polyethylene/paraffin oil blend sheets formed under non-isothermal condition

Molecular weight	$\Phi/$ $^{\circ}\text{C min}^{-1}$	hkl	$2\theta/^{\circ}$	$d/\text{\AA}$	$L/\text{\AA}$	crystallinity/ %	
						X_{XRD}	X_{DSC}
3×10^5	1	(110)	21.66	4.10	145.71	80.7	74.3
		(200)	24.13	3.69	134.01		
3×10^5	10	(110)	21.75	4.09	135.71	82.3	77.0
		(200)	24.17	3.68	134.02		
5×10^5	10	(110)	21.83	4.07	138.07	85.7	80.7
		(200)	24.21	3.67	113.27		
1×10^6	10	(110)	21.62	4.11	125.08	77.3	60.3
		(200)	24.05	3.70	118.23		

**Fig. 13** XRD patterns for polyethylene/paraffin oil blend sheets formed under different cooling rates: polyethylene of a molecular weight of 3×10^5

(110) and (200) of orthorhombic phase of polyethylene, respectively. Interplanar distance (d) can be calculated by Bragg's law [27] and lamellar thickness (L) can be calculated by Scherrer equation [28]. Values of d and L are listed in Table 6. Interplanar distance of crystal plane does not change with the increase of molecular weight of polyethylene. Interplanar distance of crystal plane (110) hovers around 4.09 Å and interplanar distance of crystal plane (200) hovers around 3.68 Å. With the increase of molecular weight of polyethylene, lamellar thickness of crystal plane decreases. This can be ascribed to the fact that polyethylene with a larger molecular weight forms less perfect crystal structure.

XRD patterns of polyethylene/paraffin oil blend sheets formed under cooling rates of 1 and 10 $^{\circ}\text{C min}^{-1}$ are compared, as shown in Fig. 13. Diffractive peaks of same crystal plane in two XRD patterns appear at almost the

same Bragg angle, which indicates that crystal structures do not change very much with change of cooling rate. Values of d and L for crystal structures formed under different cooling rates are listed in Table 6. Two crystal structures share almost the same interplanar distances. Interplanar distances of crystal plane (110) are around 4.09 Å and interplanar distances of crystal plane (200) are around 3.68 Å. The biggest difference between two crystal structures lays in lamellar thickness of crystal plane (110) which is 145.71 Å and 135.71 Å, respectively, indicating that blend sheet formed under cooling rate of 1 $^{\circ}\text{C min}^{-1}$ has more perfect crystals formed.

Crystallinity of blend sheets derived from DSC curves and XRD patterns are listed in Table 6. Variation tendency of crystallinity derived from DSC (X_{DSC}) is same as that derived from XRD (X_{XRD}). X_{XRD} is larger than X_{DSC} because measuring principle and calculation method of XRD are quite different from DSC. DSC measures the enthalpy and XRD proportions of crystal parts to amorphous parts where distinction between two parts is obscure so that some amorphous parts may be regarded as crystal parts and therefore X_{DSC} increases. Variation tendency of crystallinity for blend sheets with the change of molecular weight is same as that for neat polyethylene (see Table 1); thus, value of crystallinity for polyethylene/paraffin oil blend sheets depends totally on properties of neat polyethylene.

Conclusions

In this paper, isothermal and non-isothermal crystallization kinetics of polyethylene/paraffin oil blend sheets with polyethylene of different molecular weights were investigated. Avrami equation was adopted to analyze isothermal crystallization kinetics and did well in interpreting isothermal crystallization behaviors. Value of n in Avrami equation hovered at 2.1 and changed little with the increase of crystallization temperature T_c , indicating that crystallization structure of polyethylene was a combination of two-dimensional structure and three-dimensional structure at temperature between 115 and 112 $^{\circ}\text{C}$. $\lg Z$ increased with the decrease of crystallization temperature, meaning that crystallization rate became faster at lower temperature. $\lg Z$ decreased with the increase of molecular weight of polyethylene, which indicated that polyethylene of a larger molecular weight had a slower crystallization rate. Effective activation energy of isothermal crystallization was calculated by Friedman method. The results of ΔE showed that isothermal crystallization rate of polyethylene of a larger molecular weight and at the beginning of crystallization were more susceptible to temperature. Jeziorny method and Mo method were applied to analyze non-

isothermal crystallization. Values of n in Jeziorny method were between 2 and 3, same as isothermal crystallization. Besides, while the cooling rate increased, $\lg Z_c$ increased and n stayed almost the same. That is, crystallization rate became faster but crystallization structure did not change much. Value of $F(T)$ in Mo method increased gradually with relative crystallinity growing from 10 to 90 %, which demonstrated that it was harder and harder for crystallization while crystallization proceeded. Effective activation energy of non-isothermal crystallization was calculated too. Under non-isothermal condition, ΔE of blend sheets with different molecular weights of polyethylene were very close to each other. Polyethylene of a molecular weight of 1×10^6 had the largest ΔE in the whole range, indicating that it was less influenced by temperature than the other two under non-isothermal condition. At last, crystal structures of blend sheets formed under non-isothermal condition were analyzed by XRD analysis. Molecular weight of polyethylene and the cooling rate had slight influence on the crystal structure and crystallinity of blend sheet.

References

- Arora P, Zhang ZM. Battery separators. *Chem Rev.* 2004;104(10):4419–62.
- Huang X. Separator technologies for lithium-ion batteries. *J Solid State Electrochem.* 2011;15(4):649–62.
- van de Witte P, Dijkstra JWA, van den Berg Feijen J. Phase separation processes in polymer solutions in relation to membrane formation. *J Membr Sci.* 1996;117(1–2):1–31.
- Shi J-L, Fang L-F, Li H, Liang Z-Y, Zhu B-K, Zhu L-P. Enhanced performance of modified HDPE separators generated from surface enrichment of polyether chains for lithium ion secondary battery. *J Membr Sci.* 2013;429:355–63.
- Park MJ, Noh SC, Kim CK. Effects of the phase behavior of the diluent mixture on the microstructure of polyethylene membranes formed by thermally induced phase separation process. *Ind Eng Chem Res.* 2013;52(31):10690–8.
- Qing-Yun W, Bo-Tong L, Meng L, Ling-Shu W, Zhi-Kang X. Polyacrylonitrile membranes via thermally induced phase separation: Effects of polyethylene glycol with different molecular weights. *J Membr Sci.* 2013;437:227–36.
- Liu M, Chen D-G, Xu Z-L, Wei Y-M, Tong M. Effects of nucleating agents on the morphologies and performances of poly(vinylidene fluoride) microporous membranes via thermally induced phase separation. *J Appl Polym Sci.* 2013;128(1):836–44.
- Ma W, Zhou B, Liu T, Zhang J, Wang X. The supramolecular organization of PVDF lamellae formed in diphenyl ketone dilutions via thermally induced phase separation. *Colloid Polym Sci.* 2013;291(4):981–92.
- Wenzhong M, Jun Z, Bruggen B, Xiaolin W. Formation of an interconnected lamellar structure in PVDF membranes with nanoparticles addition via solid-liquid thermally induced phase separation. *J Appl Polym Sci.* 2013;127(4):2715–23.
- Won-Kyung S, Yoon-Sung L, Dong-Won K. Hybrid composite membranes based on polyethylene separator and Al₂O₃ nanoparticles for lithium-ion batteries. *J Nanosci Nanotechnol.* 2013;13(5):3705–10.
- Prasanna K, Lee CW. Physical, thermal, and electrochemical characterization of stretched polyethylene separators for application in lithium-ion batteries. *J Solid State Electrochem.* 2013;17(5):1377–82.
- Park MJ, Kim CK. Fabrication of polyethylene microporous membranes using triethylolpropane tris(2-ethylhexanoate) as a novel diluent by a thermally induced phase separation process. *J Membr Sci.* 2014;449:127–35.
- Kim KJ, Park M-S, Yim T, Yu J-S, Kim Y-J. Electron-beam-irradiated polyethylene membrane with improved electrochemical and thermal properties for lithium-ion batteries. *J Appl Electrochem.* 2014;44(3):345–52.
- Avrami M. Kinetics of phase change (I): general theory. *J Chem Phys.* 1939;7(12):1103–12.
- Jeziorny A. Parameters characterizing the kinetics of the non-isothermal crystallization of poly(ethylene terephthalate) determined by d.s.c. *Polymer.* 1978;19(10):1142–4.
- Ozawa T. Kinetics of non-isothermal crystallization. *Polymer.* 1971;12(3):150–8.
- Tianxi L, Zhishen M, Shanger W, Hongfang Z. Nonisothermal melt and cold crystallization kinetics of poly(aryl ether ether ketone ketone). *Polym Eng Sci.* 1997;37(3):568–76.
- Qiu ZB, Mo ZS, Yu YN, Zhang HF, Sheng SR, Song CS. Non-isothermal melt and cold crystallization kinetics of poly(aryl ether ketone ether ketone ketone). *J Appl Polym Sci.* 2000;77(13):2865–71.
- Liu TX, Mo ZS, Zhang HF. Nonisothermal crystallization behavior of a novel poly(aryl ether ketone): PEDEK_mK. *J Appl Polym Sci.* 1998;67(5):815–21.
- Zhang J, Chen S, Su J, Shi X, Jin J, Wang X, et al. Non-isothermal crystallization kinetics and melting behavior of EAA with different acrylic acid content. *J Therm Anal Calorim.* 2009;97(3):959–67.
- Wang S, Zhang J. Non-isothermal crystallization kinetics of high density polyethylene/titanium dioxide composites via melt blending. *J Therm Anal Calorim.* 2014;115(1):63–71.
- Vyazovkin S. Modification of the integral isoconversional method to account for variation in the activation energy. *J Comput Chem.* 2001;22(2):178–83.
- Achilias DS, Papageorgiou GZ, Karayannidis GR. Evaluation of the isoconversional approach to estimating the Hoffman–Lauritzen parameters from the overall rates of non-isothermal crystallization of polymers. *Macromol Chem Phys.* 2005;206(15):1511–9.
- Brandrup J, Immergut E. *Polymer handbook.* New York: Wiley; 1999.
- Liu S, Zhou C, Yu W. Phase separation and structure control in ultra-high molecular weight polyethylene microporous membrane. *J Membr Sci.* 2011;379(1–2):268–78.
- Chun-Fang Z, Yun-Xiang B, Jin G, Yu-Ping S. Crystallization kinetics of ultra high-molecular weight polyethylene in liquid paraffin during solid-liquid thermally induced phase separation process. *J Appl Polym Sci.* 2011;122(4):2442–8.
- Jauncey GE. The scattering of X-Rays and Bragg's law. *Proc Natl Acad Sci USA.* 1924;10(2):57–60.
- Cullity BD, Stock SR. *Elements of X-Ray diffraction.* New Jersey: Prentice Hall; 2001.